

ОБРАБОТКА МЕТАЛЛОВ ДАВЛЕНИЕМ

UDC 621.77

<https://doi.org/10.18503/1995-2732-2019-17-2-24-31>

3D COUPLED THERMO-MECHANICAL FE ANALYSIS OF EFFECT OF PROCESS PARAMETERS IN RING ROLLING PROCESS

Phalke Vikram¹, Nayak Soumyaranjan², Narasimhan K.², Nandedkar V.M.¹¹Shri Guru Gobind Singhji Institute of Engineering and Technology, Nanded, India²Indian Institute of Technology Bombay, Mumbai, India

Abstract. Radial-axial ring rolling is an incremental metal forming technique which is used to produce seamless rings. The advantages associated with the process include close tolerance, short production time and significant saving in material. The process marks non-uniformity in temperature and plastic strain variation. The process parameters such as mandrel feed rate, rotational speed of the main roll and axial roll feed rate have an impact on temperature and strain distribution. A coupled thermo-mechanical FE analysis is carried out in ABAQUS/Explicit to study the effect of various combinations of process parameters on the uniformity of temperature and deformation. Taguchi method is employed to find optimum process parameters. ANOVA (ANalysis Of VAriance) is carried out to assess the effect of process parameters on plastic strain and temperature.

Keywords: ABAQUS, Process Parameters, Ring rolling, Thermo-mechanical, Taguchi, ANOVA.

Introduction

Ring rolling forging is used to produce precision axis-symmetric hollow mechanical parts. The technology of ring rolling has evolved over a period of 150 years, with a significant amount of research work in the area being done in the past 40 years[1]. This process can be divided into two major types, which are, radial ring rolling (RRR) and radial-axial ring rolling (RARR). Fig. 1 shows the working principle and motion of the different rolls involved. RARR is accompanied by two compressions, one is the radial compression in between the mandrel and main roll and axial compression which takes place in between the axial rolls [2]. The main roll rotates about its own axis. Friction between the surfaces of the preform and main roll causes the preform to rotate. The mandrel is provided with a translational motion towards the main roll, the mandrel is free to rotate about its own axis because of friction. The axial rolls compress the sample in the axial direction, themselves rotating about their axes and have retrieval motion depending on the ring growth velocity [3]. Both radial and axial compression of the ring leads to decrease in the cross-sectional area which leads to circumferential extrusion of the ring and an increase in the diameter of the ring is observed.

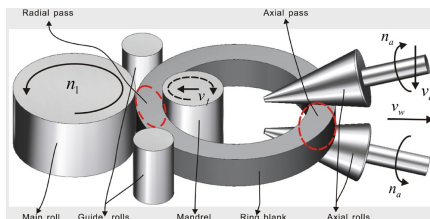


Fig. 1 Schematic of Radial-axial ring rolling process[3]

During plastic deformation of the ring, several attempts have been made to study the deformation behaviour, distribution of temperature and plastic strain of across the thickness of the ring. Zhou et al. [2] looked into the effect of changing the size of the rolls on deformation and temperature distribution. Increasing the main roll diameter, the strain distribution of the rings rolled becomes furthermore non-homogenous while the distribution of temperature became more uniform. On increasing the mandrel diameter, uniformity in the strain distribution is seen first followed by a decrease in uniformity later, whereas the temperature distribution becomes more non-uniform. Zhou et al. [4] looked into the plastic and temperature distribution across the thickness of the ring using

FE simulation. The plastic strain decreases from the ring surface to the centre of the cross section of

© Phalke Vikram, Nayak Soumyaranjan, Narasimhan K., Nandedkar V.M., 2019

the ring, while the reverse trend observed in temperature distribution.

Li et al. [8] developed 3D thermo-mechanically coupled FE model to analyse the effect of feed speed of rolls on the outer and inner diameter of the ring and plastic strain distribution across the ring thickness. Berti et al. [9] used FE simulation to determine the stable kinematic condition of different process parameters such as main roll rotation speed, mandrel feed rate etc. and to determine initial dimensions of the preform. Yang et al. [10] developed 3D FE – model to study the movement and position of guide roll in order to form precise quality rings. Zhou et al. [11] developed a finite element model of the RARR process to look into the effects of lubrication conditions and feed rate on temperature and strain distributions and their uniformity across the thickness of the ring. Giorleo et al. [12] looked into the effect of preform height on energy and force required in upsetting, piercing and during ring rolling process using FE modeling.

In the present study, effect of the combination of different process parameters on distribution of temperature and plastic strain is studied using thermo-mechanically coupled FE model developed in ABAQUS/Explicit. Taguchi method is used to find the optimal process parameters in the ring rolling process and analysis of variance (ANOVA) is carried out to find the impact of each process parameters.

Stable forming conditions

1. Rotational Speed of Main Roll (n_1) and Axial Roll (n_{a1})

The actual ring rolling process the linear speed of ring should be kept within the range of 0.4 to 0.6 m/sec to guarantee stability of rolling process [4]

The range rotational speed of the main roll is given by the following equation:

$$\frac{0.4}{R_1} < n_1 < \frac{0.6}{R_1} \quad (1)$$

Axial rolls rotational speed (n_{a1}) corresponding to the main roll can be calculated as follows [3]

$$n_{a1} = \frac{R_1 n_1}{R_{a1}} \quad (2)$$

2. Feed Speed of Mandrel (V_f) and axial rolls (V_a):

The feed speed ranges of the axial roll and mandrel depend on the draft (Δh), the radius of the main roll (R_1), the rotation speed of main roll (n_1), and initial (D_0) and final (D_f) diameter of the ring [3]:

$$\frac{2\Delta h_{min} R_1 n_1}{D_0} \leq V_f \leq \frac{2\Delta h_{max} R_1 n_1}{D_f} \quad (3)$$

$$\frac{2\Delta h_{min} R_1 n_1 (b_0 - b_f)}{D_0 (h_0 - h_f)} \leq V_a \leq \frac{2\Delta h_{max} R_1 n_1 (b_0 - b_f)}{D_f (h_0 - h_f)} \quad (4)$$

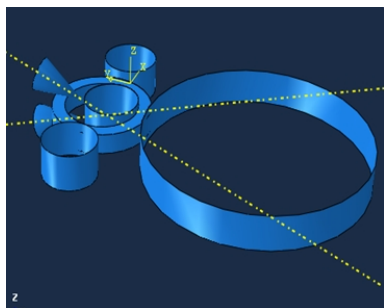
3D Finite Element modelling

In order to predict the influence of the combination of different process parameters on ring rolling process a 3D FE model is developed in ABAQUS/Explicit.

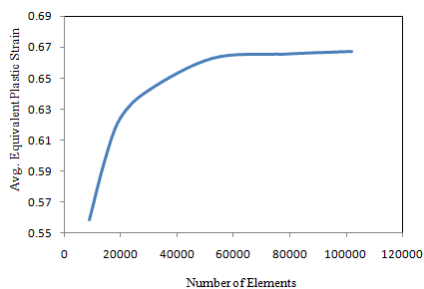
A thermo-mechanical coupled model with 8 nodes hexahedron elements (C3D8RT) is effectively used to simulate high-temperature ring rolling process as shown in **fig. 2 (a)**. The convergence study is carried out in order to decide an optimum number of elements as shown in **fig. 2 (b)**. The mass scaling and hourglass control is used to reduce computation time. The adaptive meshing technique is used to preserve the quality of mesh during the simulation. Heat convection coefficient; heat radiation coefficient and thermal contact conductance are defined in order to envisage the temperature variation of the ring with respect to rolling time. The initial temperature of the workpiece is assigned in 'predefined field' in ABAQUS at each node of the element. The workpiece is treated as deformable body and rolls as analytical rigid bodies. The Point mass and rotary inertia are defined to rigid bodies. The coefficient of friction is defined between the mandrel, main roll, axial rolls and the ring surface. The interaction amongst guide rolls and workpiece is kept as frictionless. The local coordinate system (rectangular) is defined and boundary conditions are applied on this coordinate system to control the movement of axial rolls. The developed FE model is validated with the model developed in Guo et al [3] for radial and axial force variation with respect to time.

Model validation

Table 1 shows the geometrical and process parameters. **Fig. 3** shows the variation of axial and radial force with respect to time. Predicted forces by simulation are measured with the simulation and experimental done by Guo et. al [3] and it is found that the simulation results and experimental results are in good agreement. There is an error in experimental and simulation data to some extent. This variation is due to material properties, friction between the rollers, the measurement technique used for force in experiment etc.



(a)



(b)

Fig. 2 a) Model developed in ABAQUS
b) Convergence study

Table 1

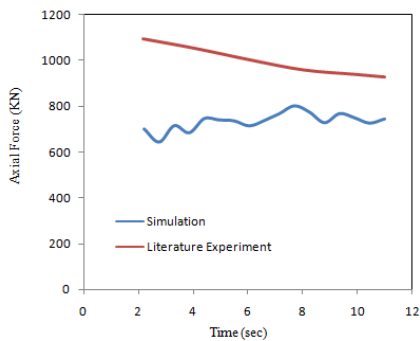
Geometrical and Process Parameters[3]

Process Parameters	Value
Outer diameters of the preform D_o , mm	483.1
Inner diameter of the preform d_o , mm	360
Height of the preform h_o , mm	84.8
Radius of the main roll R_1 , mm	550
Radius of the mandrel R_2 , mm	130
Taper angle of the axial rolls θ^0	35
Radius of the axial rolls R_{a1} , mm	72.6
Initial temperature of the ring, 0C	1020
Temperature of the rigid bodies, 0C	300
Temperature of the environment, 0C	20
Rotation speed of the main roll, n_1 (rad/sec)	1.5
Feed rate of the mandrel, V_f (mm/sec)	0.98

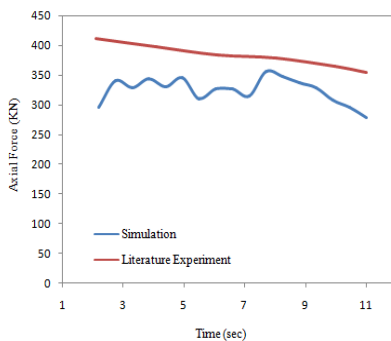
The selection of process parameters

In order to produce a stable forming condition, there is certain upper and lower limit for process parameters as mentioned in equation 1 to 4. For the above validated model, the range of feed rates of the mandrel is $V_f \in (0.1087, 1.60)$. The range for feed rates of axial roll is $V_a \in (0.07, 0.82)$, and the range for rotation speed of the main roll is $n_1 \in (0.72, 2.90)$.

In the present study combination of different process, parameters are taken into account to find the effect of these process parameters on the distribution of strain and temperature. The parameters chosen for study are in the range of stable forming condition as shown in Table 2.



(a)



(b)

Fig. 3 a) Axial and b) Radial force variation with respect time

Table 2

Parameters chosen for study

V_f (mm)	0.5	0.98	1.47
V_a (mm)	0.4	0.67	0.8
n_1 (rad/sec)	0.75	1.5	2.25

Results and Discussion

1. Plastic Strain and temperature Distribution

The Simulations were carried out with L_9 orthogonal array. **Fig. 4** shows the distribution of equivalent plastic strain (PEEQ) and temperature in the cross-section of the ring. From the **fig. 4** it can be found that PEEQ and temperature distribution is not uniform along the thickness of the ring. The maximum PEEQ found at the ring's outer and inner surface while it is minimum at the center region of the cross-section, the reason for this is that the ring is more plastically strained at the surface then at the bulk of the ring. The ring temperature is also non-homogenous; it increases from the outer surface of the ring to central region along thickness and again decreases from central portion to inner surface the ring. The reason for this is maximum heat loss takes from the surface of the ring due convection, radiation and due to thermal contact conductance between the rolls and the ring and deformation heat also adds to the temperature of the central region.

2. Quantifying Uniformity of Deformation and Temperature

In order to quantify the degree of deformation and temperature, the standard deviation can be calculated using the following formula[4]:

$$SD = \sqrt{\left(\frac{\sum_{i=1}^n (X_i - X_a)^2}{N} \right)} \quad (6)$$

Where X_i is the value of PEEQ or temperature at the i^{th} element, X_a is the average value of all the elements and N is the total number of elements considered.

3. Design of Experiment and Taguchi Method

Taguchi method is an optimisation technique which is widely used in engineering analysis. The quality characteristic used here is:

Smaller-is-better (minimize),

$$[S/N]_{SB} = -10 \log \left(\frac{1}{n} \sum_{i=1}^n y_i^2 \right) \quad (7)$$

Where the n is number of observation and y is the observed data.

In the present work, the objective was to minimise standard deviation for strain and temperature so smaller-is-better quality characteristic was used. Three process parameters: mandrel feed rate (D) mm/s, axial roll feed speed (E) mm/s and main roll rotational speed (F) rad/s with three levels were used and is shown in **Table 2**.

The three values of response (SDP and SDT) were calculated at three cross-sections of the ring 90° apart as shown in **Table 3**. The average values of response were taken for further calculations. The signal to noise ratio (S/N) were found out by using smaller to better quality characteristic as shown in **Table 4**. The average S/N ratio values of the three factors at each different levels are shown in **Fig. 5**. The peak S/N ratio values were taken for each process parameter which represents the optimum condition [17]. It has been observed from the **fig. 5(a)** that optimal combination of parameters involved in the process for uniform distribution of equivalent plastic strain is $D_3E_3F_1$. It has been observed that the optimal combination of parameters involved in the process for uniform temperature distribution is $D_3E_2F_3$ in **fig. 5(b)**.

Table 3

Average SDP, SDT and S/N ratio

Simulation No.	SDP			SDT		
1	0.3548	0.3714	0.3416	6.5253	6.3346	6.6227
2	0.6845	0.6346	0.6820	6.2648	6.2987	6.1446
3	0.9081	0.8483	0.7633	5.4047	5.2502	5.2704
4	0.6343	0.6387	0.6167	4.8503	4.7931	4.9440
5	0.5015	0.4870	0.458	4.8925	4.8943	4.9515
6	0.3010	0.3221	0.2020	5.3471	5.1778	5.2046
7	0.3983	0.4186	0.3473	5.5300	4.3270	4.3731
8	0.5377	0.4809	0.4883	3.8095	3.7995	3.8295
9	0.2223	0.3619	0.1902	4.4404	4.4579	4.4616

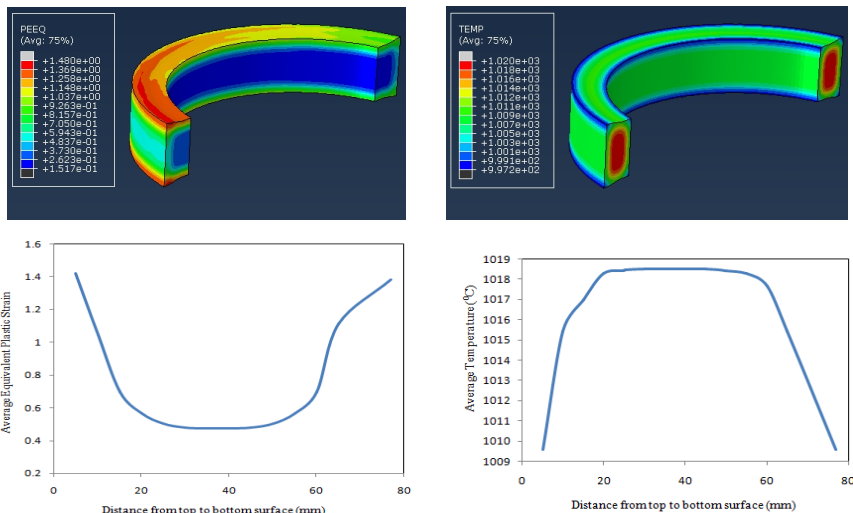


Fig. 4. PEEQ and Temperature distribution

Table 4

Average SDP, SDT and S/N ratio

Simulation No.	Average SDP	S/N Ratio	Average SDT	S/N Ratio
1	0.3559	8.9669	6.4942	-16.2505
2	0.6670	3.5118	6.2360	-15.8982
3	0.8399	1.4937	5.3084	-14.4993
4	0.6299	4.0135	4.8624	-13.7371
5	0.4821	6.3298	4.9127	-13.8265
6	0.2750	11.0563	5.2431	-14.3919
7	0.3880	8.1957	4.7433	-13.5217
8	0.5023	5.9692	3.8128	-11.625
9	0.2581	11.4145	4.4533	-12.9736

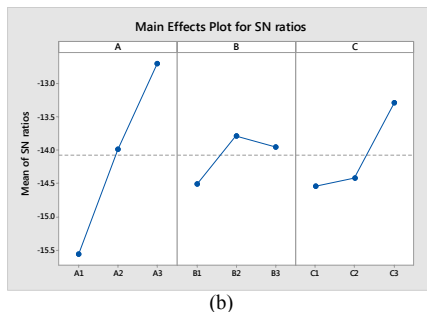
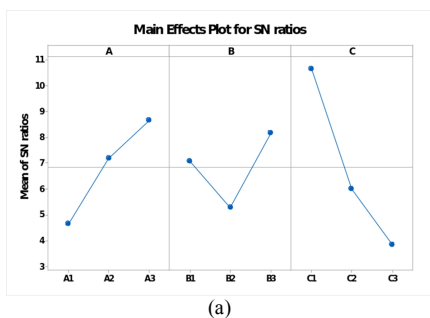


Fig. 5 Mean of S/N ratio for a) strain distribution
b) temperature distribution

4. Confirmation Test

The optimal combination of parameters involved in the process has been determined using Taguchi method. The confirmation test is carried out to determine and verify observed data by using optimum combination of process parameters. The optimum parameters for strain lie in the L_9 orthogonal array; therefore confirmation test is not mandatory for strain distribution. The confirmation test is carried out for optimum parameters $A_3B_2C_3$ for temperature distribution. The percentage error of 0.65% found in between mathematical equation and in an actual run.



$$\text{Optimal value} = Y' + (D' - Y') + (E' - Y') + (F' - Y') \quad (8)$$

$$Y' = \frac{T}{N} \quad (9)$$

Where,

Y' : Average of total response value

T : total of average SDT for each simulation

N : number of simulations

$D', E' \wedge F'$: Average values of SDT and SDP for process parameter at their respective optimal level

Table 5

Confirmation Test

Sr. No	The optimum value of SDT by Eq.	Optimum value of SDT by actual run	% Error
1	3.7139	3.7383	0.65

5. Analysis of variance (ANOVA)

ANOVA method is used to explore the significance of parameters involved in the process in terms of percentage contribution. This analysis is carried out at 95% confidence level and 5% significance level. The last column of the ANOVA table 7 demonstrates the contribution of each process parameter in terms of percentage, which indicates the influence of each process parameters on the response. The total sum of the squared deviation is given by the following equation [18]

$$SS_T = \sum_{i=1}^n y_i^2 - C.F. \quad (10)$$

Where n is the number of simulations in the orthogonal array, y_i is the response for i^{th} simulation and $C.F.$ is the correction factor.

$C.F.$ can be calculated as [18]:

$$C.F. = \frac{T^2}{n} \quad (11)$$

T is the total of the response.

In ANOVA table, the contribution of each process parameter is calculated by dividing the sum of squared deviation for each parameter by the total sum of squared deviation. The mean of the squared deviation is found out by dividing the sum of squared deviation by a number of degrees of freedom (DOF). Fisher test (F-value) is carried out to find which process parameter has a significant effect on response.

Table 6 shows the outcomes of ANOVA for plastic strain distribution.

5.1. ANOVA for PEEQ

Table 6

Analysis of variance for PEEQ

Source	DF	Sum of Square	Mean Square	F-Value	% C
Mandrel Feed Speed (mm/s)	2	0.0881	0.0440	20.28	29.21
Axial Roll Speed (mm/s)	2	0.0113	0.0056	2.66	3.75
Main Roll Rotation Speed (r/s)	2	0.1921	0.0960	44.20	63.65
Error	2	0.0043	0.0021		3.38
Total	8	0.3018			

5.2. Analysis of Variance for temperature

Table 7

Analysis of variance for temperature

Source	DF	Sum of square	Mean Square	F-Value	%C
Mandrel Feed Speed (mm/s)	2	4.2718	2.1359	55.97	76.44
Axial Roll Speed (mm/s)	2	0.2843	0.142	13.73	5.08
Main Roll Rotation Speed (r/s)	2	0.9629	0.4814	12.62	17.23
Error	2	0.0763	0.0381		1.25
Total	8	5.5884			

It can be concluded that the main roll rotation speed has the largest contribution of 63.65% in uniform plastic strain distribution, mandrel feed speed has the contribution of 29.21% and axial roll feed speed has least contribution of 3.756%. Table 7 shows the outcomes of ANOVA for temperature distribution. It can be concluded that mandrel feed speed has the largest contribution of 76.44% in uniform temperature distribution, main roll rotation speed has the contribution of 17.23% and axial roll feed speed has the contribution of 5.08%

Conclusion

The effect of combinations of various process parameters on the degree of deformation and temperature distribution were studied using FE analysis. It can be concluding that:

1. The optimum combination of process parameters for uniform stain and uniform temperature distribution are $D_3E_3F_1$ and $D_3E_2F_3$ respectively was found out using Taguchi method.
2. From ANOVA, the contributions of process parameters for uniform stain distribution and temperature distribution is main roll rotation speed (n_1) > mandrel feed speed (V_f) > Axial roll feed speed (V_a) and mandrel feed speed (V_f) > main roll feed speed (n_1) > axial roll feed speed (V_a) respectively.

References

1. J.M. Allwood, E. Tekkaya, and T.F. Stanistreet. The development of ring rolling technology. *Steel Research International*, 2005, no. 2–3, pp. 111–120.
2. G. Zhou, L. Hua, and D.S. Qian. 3D coupled thermo-mechanical FE analysis of roll size effects on the radial-axial ring rolling process. *Computational Material Science*, 2011, vol. 50, no. 3, pp. 911–924.
3. L. Guo and H. Yang. Towards a steady forming condition for radial-axial ring rolling. *International Journal of Mechanical Science*, 2011, vol. 53, no. 4, pp. 286–299.
4. G. Zhou, L. Hua, J. Lan, and D.S. Qian. FE analysis of coupled thermo-mechanical behaviors in radial-axial rolling of alloy steel large ring. *Computational Material Science*, 2010, vol. 50, no.1, pp. 65–76.
5. L. Giorleo, E. Ceretti, and C. Giardini. Milling Curves Influence in Ring Rolling Processes. *Key Engineering Materials*, 2014, vols. 622–623, pp. 956–963.
6. X. Wang and L. Hua. Analysis of guide modes in vertical hot ring rolling and their effects on the ring's dimensional precision using FE method. *Journal of Mechanical Science and Technology*, 2011, vol. 25, no. 3, pp. 655–662.
7. D.R. Nielsen, S.W. Thompson, C.J. Van Tyne, and M.C. Mataya. Grain Size Control in Ring-Rolled Alloy 718. *The Minerals, Metals & Materials Society*, 1994, pp. 373–392.
8. Q. Li, Z. Ma, T. Liu, F. Li, Z. Wei, and C. Su. 3D thermomechanically coupled FEM analysis of large disk rolling process and trial production. *International Journal of Advanced Manufacturing Technology*, 2014, vol. 74, no. 1–4, pp. 403–411.
9. G. A. Berti, L. Quagliato, and M. Monti. Set-up of radial-axial ring-rolling process: Process worksheet and ring geometry expansion prediction. *International Journal of Mechanical Science*, 2015, vol. 99, pp. 58–71.
10. L.Li, H. Yang, L. Guo, and Z. Sun. A control method of guide rolls in 3D-FE simulation of ring rolling. *Journal of Materials Processing Technology*, 2008, vol. 205, no. 1–3, pp. 99–110.
11. J. Zhou, F.L. Wang, M.H. Wang, and W.J. Xu. Study on forming defects in the rolling process of large aluminum alloy ring via adaptive controlled simulation. *International Journal of Advanced Manufacturing Technology*, vol. 55, no. 1–4, 2011.
12. L. Giorleo, E. Ceretti, and C. Giardini. Energy consumption reduction in Ring Rolling processes: A FEM analysis. *International Journal of Mechanical Science*, 2013, vol. 74, pp. 55–64.
13. H. Lin and Z. Z. Zhi. The extremum parameters in ring rolling. *Journal of Materials Processing Technology*, 1997, vol. 69, no. 1–3, pp. 273–276.
14. M. Kaladhar, K.V. Subbaiah, and C.H.S. Rao. Optimization of surface roughness and tool flank wear in turning of AISI 304 austenitic stainless steel with cvd coated tool. *Journal of Achievements in Materials and Manufacturing Engineering*, 2013, vol. 8, no. 2, pp. 165–176.
15. K. Universiti, T. Tun, and H. Onn. Analyses of surface roughness by turning process using Taguchi method. *Journal of Achievements in Materials and Manufacturing Engineering*, 2007, vol. 20, no. 1–2, pp. 503–506.
16. T. Kivak. Optimization of surface roughness and flank wear using the Taguchi method in milling of Hadfield steel with PVD and CVD coated inserts. *Measurement*, 2014, vol. 50, pp. 19–28.
17. N. Mondal, B. Doloi, B. Mondal, R. Das. Optimization of Flank wear using Zirconia toughened Alumina (ZTA) cutting tools: Taguchi Method and Regression Analysis. *Measurement*, 2011, vol. 44, no. 10, pp. 2149–2155.
18. S. Kamaruddin, Z.A. Khan, K.S. Wan, and N. Tebal. The use of the taguchi method in determining the optimum plastic injection moulding parameters for the production of a consumer. *Jurnal Mekanikal*, 2004, vol. 18, pp. 98–110.

Received 15/01/19

Accepted 14/02/19

ИНФОРМАЦИЯ О СТАТЬЕ НА РУССКОМ

УДК 621.77

<https://doi.org/10.18503/1995-2732-2019-17-2-24-31>

ОБЪЕМНЫЙ СОПРЯЖЕННЫЙ ТЕРМОМЕХАНИЧЕСКИЙ КЭ-АНАЛИЗ ВЛИЯНИЯ ТЕХНОЛОГИЧЕСКИХ ПАРАМЕТРОВ ПРОЦЕССА РАСКАТКИ КОЛЕЦ

Фальке Викрам¹, Найак Сумяраян², Нарасимхан К.^{2*}, Нандедкар В.М.¹

¹ Инженерно-технологический институт Шри Гуру Гобинд Сингх-джи, Нандед, Индия

² Индийский технологический институт Бомбей, Мумбай, Индия. E-mail: nara@iitb.ac.in

Аннотация. Радиально-аксиальная раскатка колец представляет собой метод ступенчатого деформирования, применяемый при изготовлении бесшовных колец. Преимущества данного метода заключаются в высокой точности изготовления, кратковременном производственном цикле, а также значительной экономии материала. При этом отмечается неравномерность температуры и колебания пластической деформации. Технологические параметры, такие как скорость подачи раскатки, скорость вращения главного валка и скорость осевой подачи валка, оказывают влияние на распределение температуры и деформа-

ций. Для изучения воздействия различных комбинаций технологических параметров на равномерность температуры и деформаций с помощью комплекса ABAQUS/Explicit проводится сопряженный термомеханический КЭ-анализ. Для определения оптимальных технологических параметров применяется метод Тагути. Для оценки влияния технологических параметров на пластическую деформацию и температуру проводят анализ ANOVA, или дисперсионный анализ.

Ключевые слова: комплекс ABAQUS, технологические параметры, раскатка колец, термомеханический, Тагути, анализ ANOVA.

Поступила 15.01.19

Принята в печать 14.02.19

•
For citation

Phalke V., Nayak S., Narasimhan K., Nandedkar V.M. 3D Coupled Thermo-Mechanical FE analysis of effect of process parameters in ring rolling process. *Vestnik Magnitogorskogo Gosudarstvennogo Tekhnicheskogo Universiteta im. G.I. Nosova* [Vestnik of Nosov Magnitogorsk State Technical University]. 2019, vol. 17, no. 2, pp. 24–31. <https://doi.org/10.18503/1995-2732-2019-17-2-24-31>

•
Образцы для цитирования

Phalke V., Nayak S., Narasimhan K., Nandedkar V.M. 3D Coupled Thermo-Mechanical FE analysis of effect of process parameters in ring rolling process // Вестник Магнитогорского государственного технического университета им. Г.И. Носова. 2019. Т.17. №2. С. 24–31. <https://doi.org/10.18503/1995-2732-2019-17-2-24-31>
•